

Supporting Information

Highly Efficient *In vivo* Editing of Macrophages through Systemic Delivery of CRISPR-Cas9-Ribonucleoprotein-Nanoparticle Nanoassemblies

*Yi-Wei Lee[†], Rubul Mout[‡], David C. Luther, Yuanchang Liu, Laura Castellanos-García, Amy S. Burnside, Moumita Ray, Gulen Yeşilbag Tonga, Joseph Hardie, Harini Nagaraj, Riddha Das, Erin L. Phillips, Tristan Tay, Richard W. Vachet and Vincent M. Rotello**

SUPPORTING NOTES

Cas9E20 sequence: (E20 at the N-terminus represents E-tag; NLS is underlined at the C-terminus)

SUPPORTING FIGURES

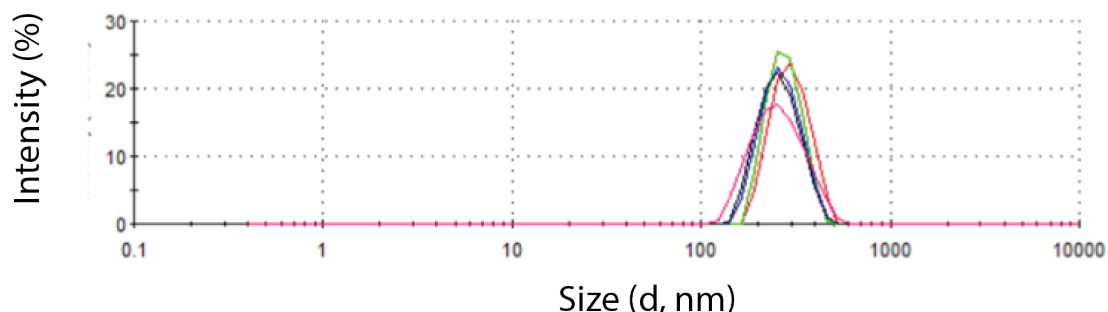


Figure S1. DLS characterization of Cas9En-RNP/AuNPs composites. Intensity histogram of composite hydrodynamic size ($n=5$). Zeta potential consistently remained between 0 and -5.

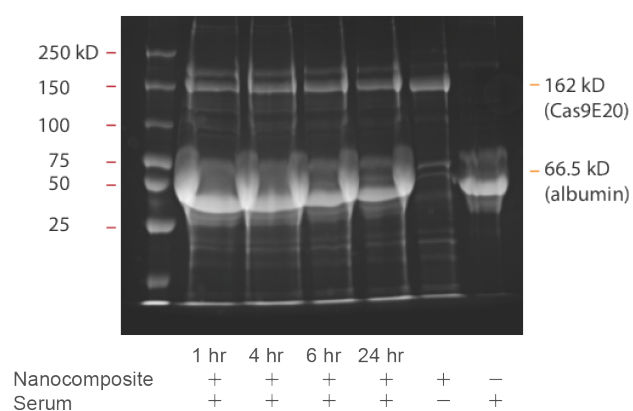


Figure S2. Serum stability test of nanocomposites in the presence of serum over a 24-hour period.

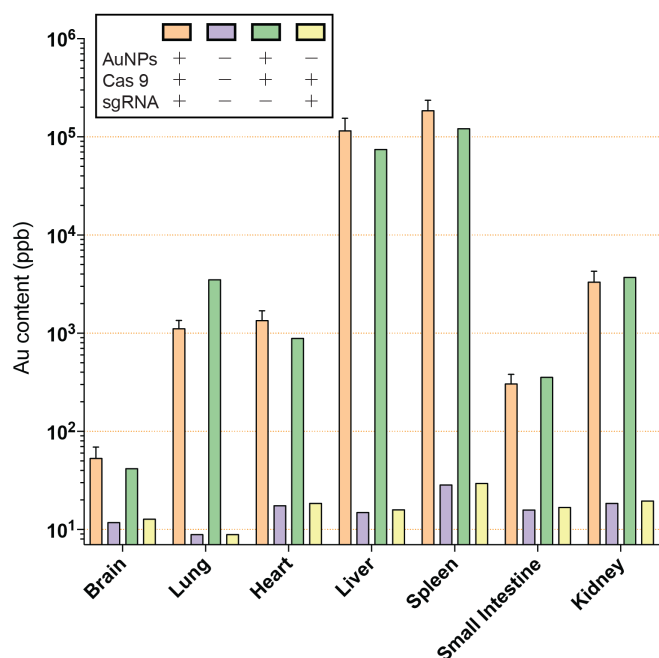


Figure S3. Biodistribution of gold in mouse different organs, quantitatively analyzed by ICP-MS. Delivery vehicle (+++) $n=3$, controls $n=1$.

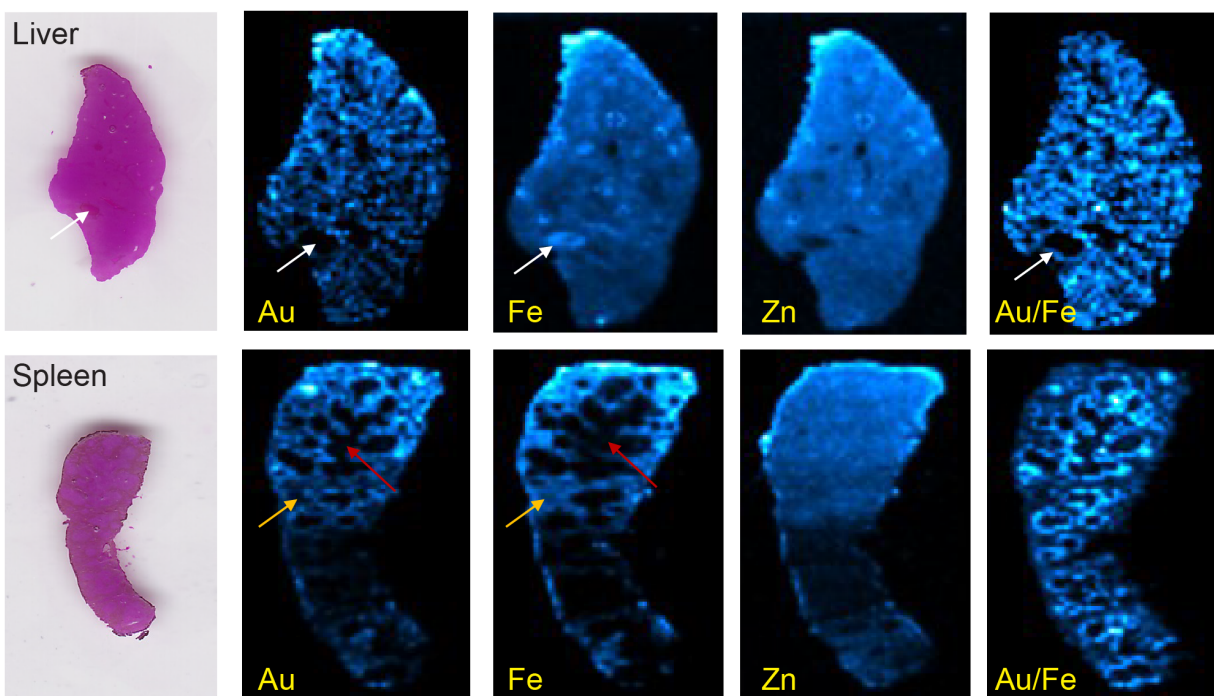


Figure S4. LA-ICP-MS and optical images of liver and spleen mouse organs of mouse injected with nanocomposites. Optical images are shown with ^{197}Au , ^{57}Fe , and ^{66}Zn metal distribution images, Au/Fe distribution is also shown. White arrows signal a vein; yellow arrows signal the red pulp while red arrows show the white pulp. The high sensitivity and spatial resolution of this technique allows us to determine how nanocomposites distribute *in vivo*.

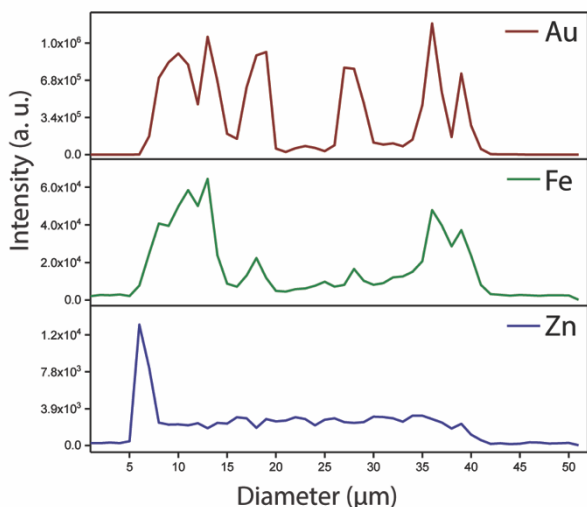


Figure S5. Single line scans of the spleen. The similarity of gold and iron indicates that the gold nanocomposites co-localized with the red pulp.

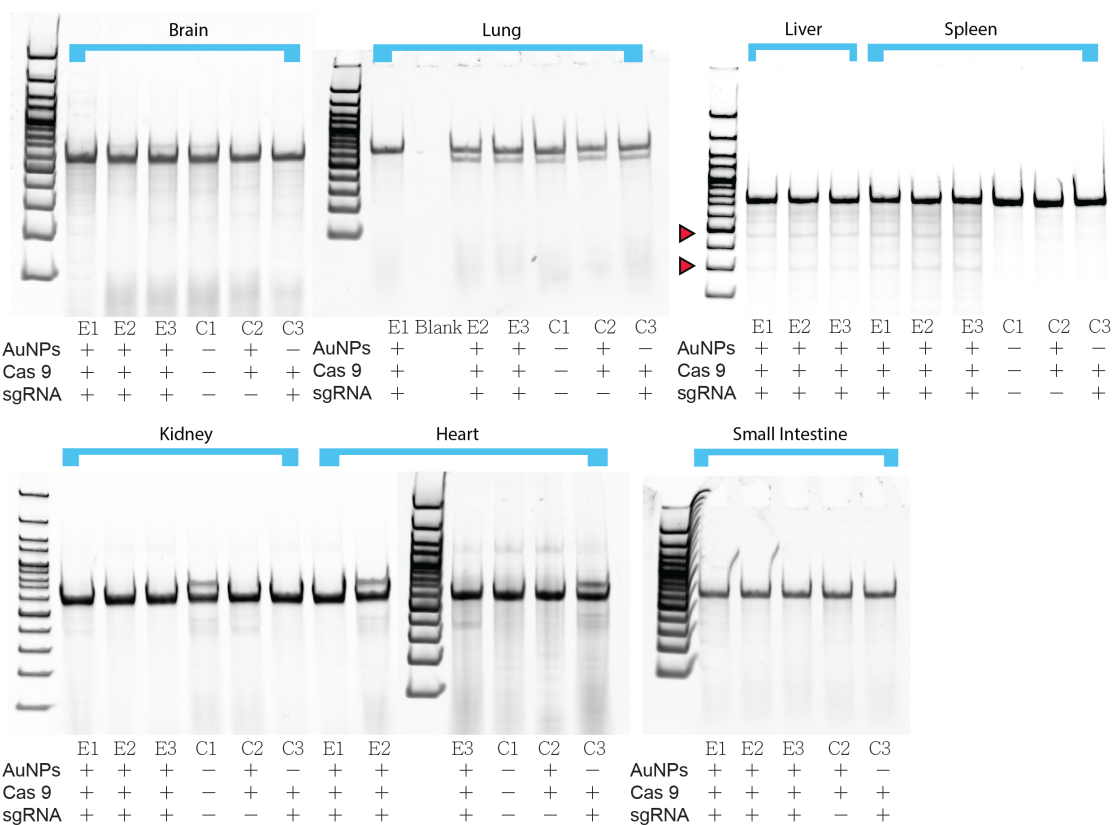


Figure S6. Efficient gene editing selectively present in organ homogenates resulting from Cas9En-RNP delivery. Experimental conditions and control conditions were shown as En and Cn. The red arrows indicate the two cutting bands after activities of the T7E1 assay.

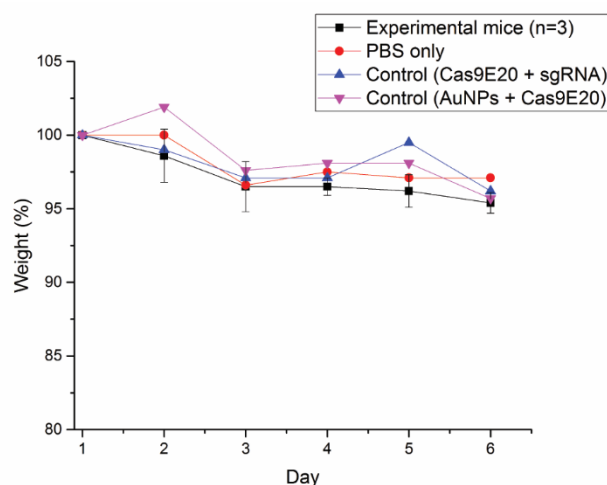


Figure S7. Quantitative tracking of weight change in mice throughout 6-day experiment.

Table S1. Primer sequences.

ID	Sequence (5'->3')
surv-PtenF	AAACCTCCCGTCCGCCGCCGC
surv-PtenR	ACCAGGCAAGAGTTCCGTCTAGCCAAACAC
PTENoff1-F	TCAGACTTCCGTGCAGTCT

PTENoff1-R	ACAAGCGGAAACATCCACAC
PTENoff2-F	TGGACTCTGCTTGAGACA
PTENoff2-R	ATAAGCCCTGGTAAGAGCC
PTENoff3-F	TCCCAGTTCTTCCCAACCTC
PTENoff3-R	ACACACGTTCAGTTCTGCC
PTENoff4-F	CCAACTCACCCCTCTCCCTT
PTENoff4-R	ACCTTGTGTGAGACTCCCCA

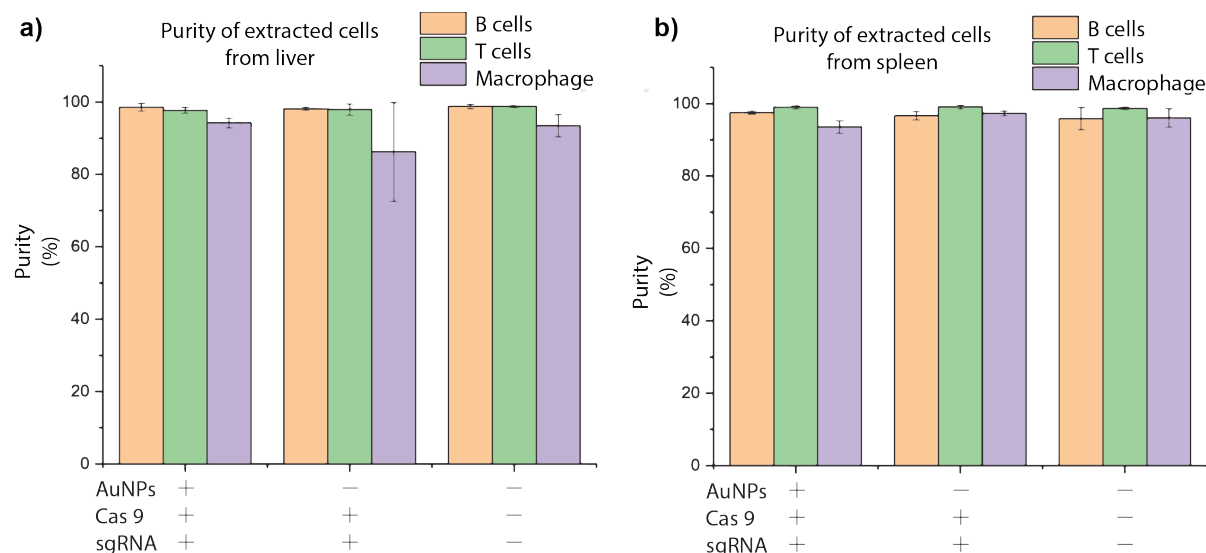


Figure S8. % purity of extracted immune cells from (a) liver and (b) spleen.

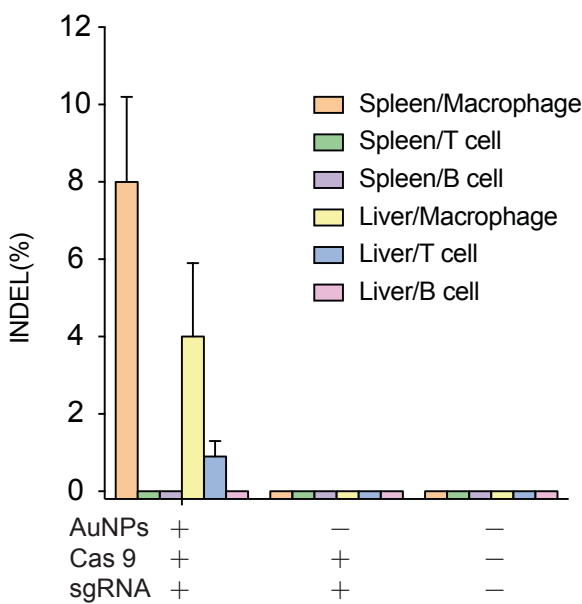
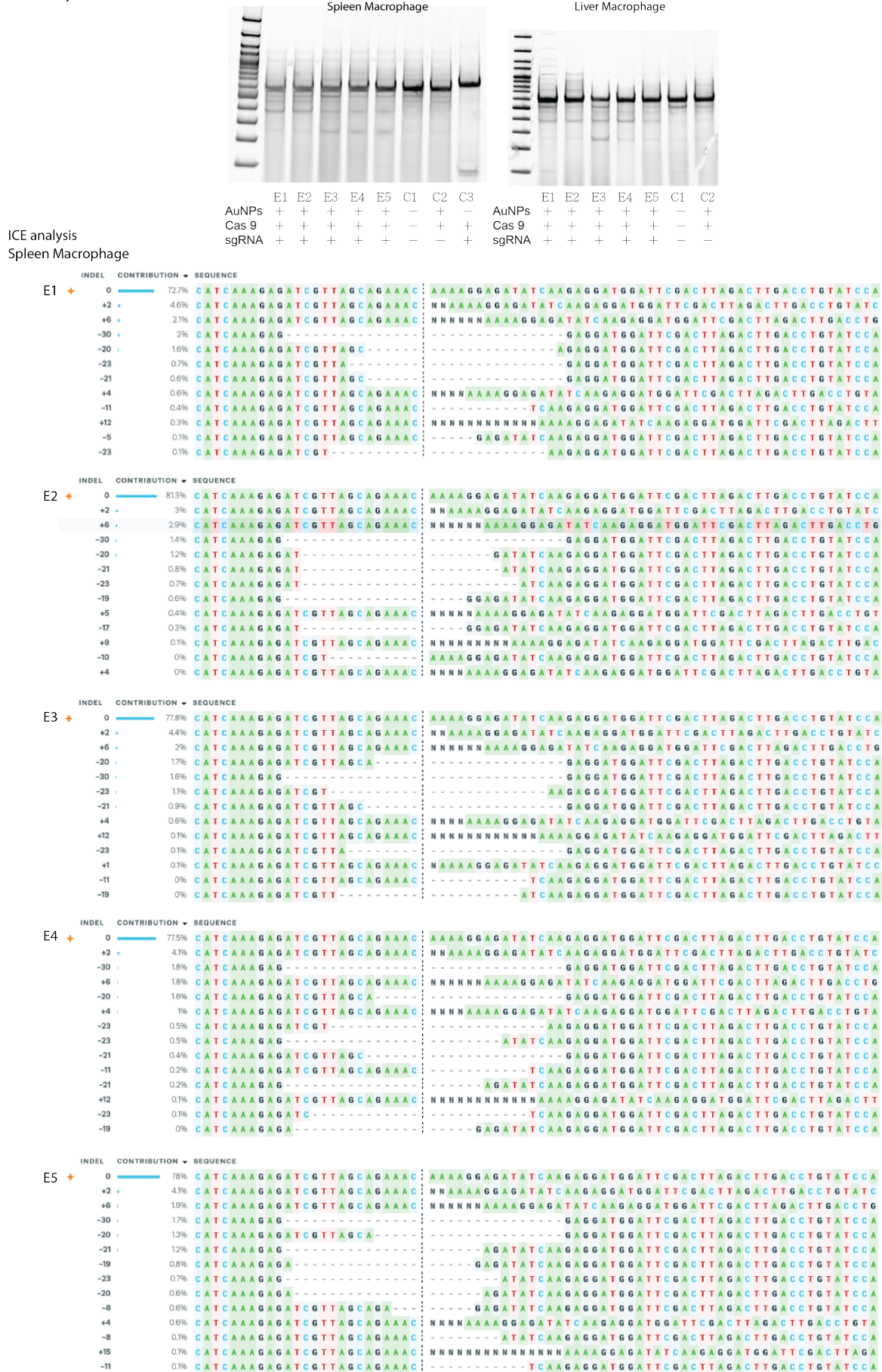


Figure S9. Insertion/deletion (indel) frequencies were observed in splenic and hepatic macrophages specifically, as analyzed by T7E1 assay.

T7E1 analysis



Liver Macrophage

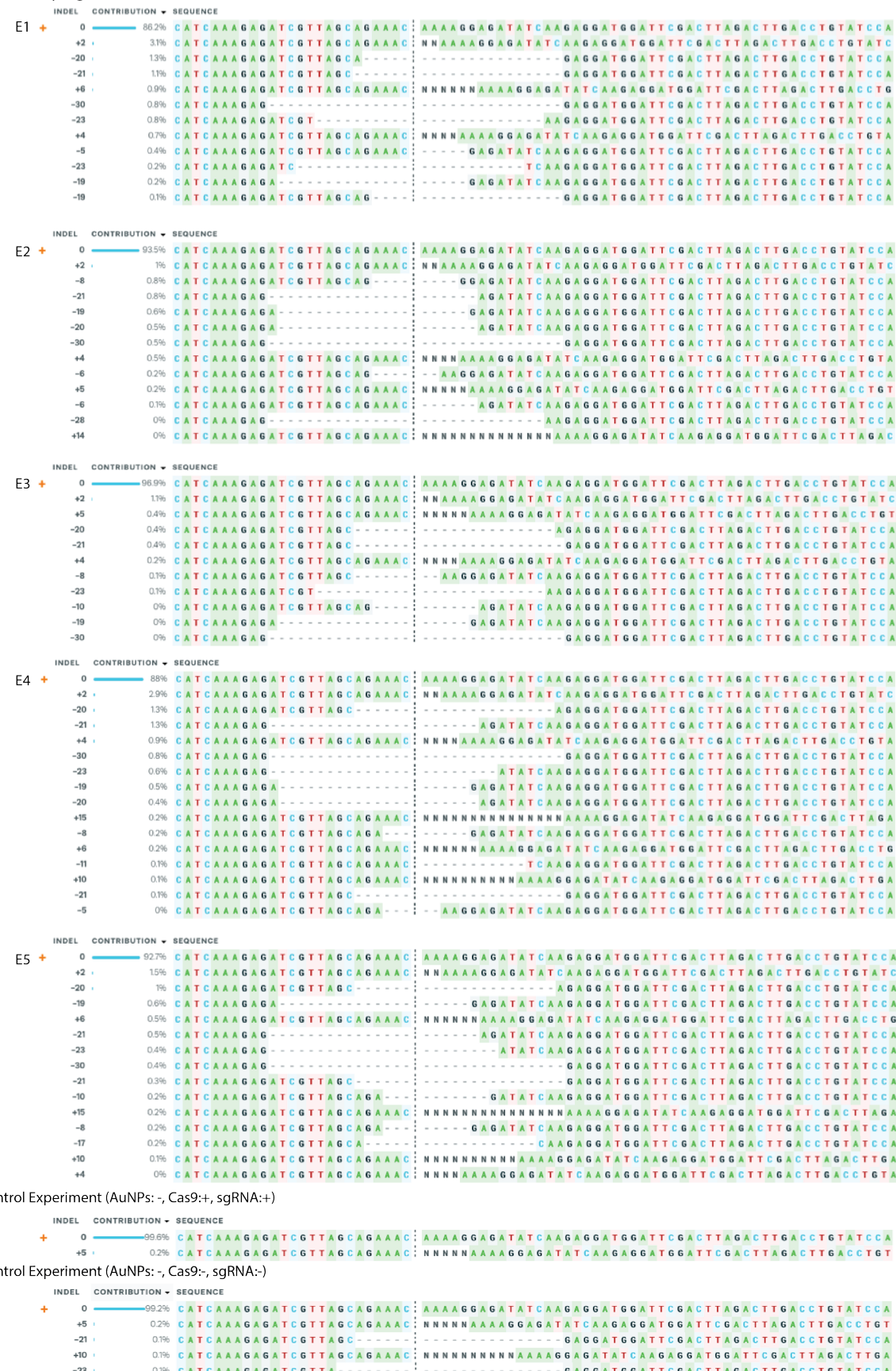


Figure S10. T7E1 gel and normalized contributions of each sequence obtained from Interference for CRISPR Edits (ICE) analysis. Experimental conditions and control conditions

were shown as En and Cn. Dash line indicates the expected cutting site; orange plus indicates the wild-type sequence.

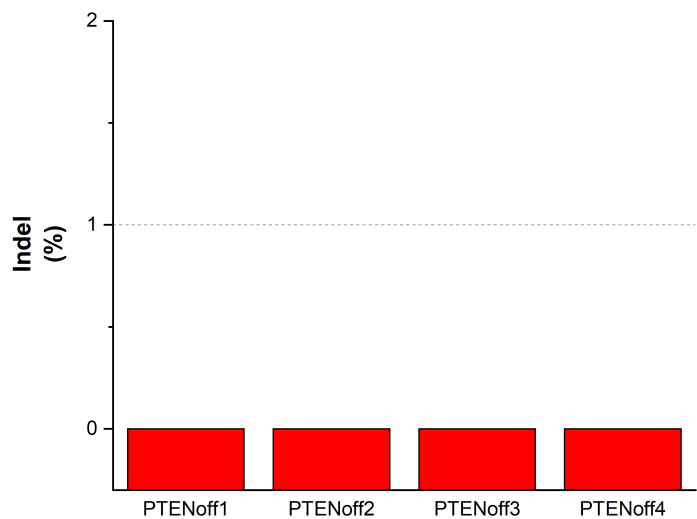


Figure S11. Off-Target editing results for the *PTEN* gene at 4 loci as measured by T7E1 assay.